DEPARTMENT OF CHEMICAL AND MATERIALS ENGINEERING

FINAL YEAR REPORT

Calibrating a Network Analyser and Microstrip Patch Antenna for Kiwifruit Ripeness Determination

---

Author:
Leah AGUSTIN

Supervisor:
Dr. Alisyn NEDOMA

October 20, 2018

UNIVERSITY OF AUCKLAND

Abstract

Faculty of Engineering

Department of Chemical and Materials Engineering

Calibrating a Network Analyser and Microstrip Patch Antenna for Kiwifruit Ripeness Determination

by Leah AGUSTIN

The following report aims to validate the use of radio-frequency (RF) waves as a potential, non-destructive method of measuring kiwifruit ripeness. Kiwifruit export has a significant contribution to New Zealand's horticultural industry. As the country's leading horticultural sector, it is therefore necessary to explore novel, non-destructive measurement methods for fruit ripeness; to improve accuracy and reduce consumable wastage.

Validation of the simulated RF data for a developed microstrip antenna involved the creation of five synthetic testing models of varying agarose concentration, soluble solids concentration (ssC) and sample thickness. Reflection coefficient values, S11, were gathered using the Vector Network Analyser (VNA) and developed microstrip patch antennas. Elastic modulus measurements were gathered using the CT3 Texture Analyser. Sources of errors throughout these analyses were reduced through repeated trials and calculation of standard errors.

The results indicate that binary agarose-glucose hydrogels demonstrate greater potential for more accurate fine-tuning of specific viscoelastic properties, in comparison to pure agarose hydrogels. A p-value of 0.3 — obtained from a t-test — indicated negligible differences between the simulated S11 data and experimental results with binary hydrogels. Despite showing promising results for each property studied, no statistically significant correlation is found between the two properties. Thus, current industrial firmness measurement methods do not provide any indication of the validity of the RF data.

Several factors, such as the lack of pre-existing literature on kiwifruit viscoelastic and dielectric properties, limit the validity of the observed results from this study. Further investigation is therefore required to allow the future commercial implementation of this non-destructive method.

Acknowledgements

I would like express my sincere gratitude to the following people who have made a significant contribution to the overall success of this project:

Dr Alisyn Nedoma, for providing an endless amount of support and guidance throughout the duration of my project

Alvin Huang and Tristan Newhook, for their hard work on the development of the microstrip patch antennas used in this investigation

Peter McAtee from the Plant and Food Research Institute, for providing expert knowledge on New Zealand's kiwifruit industry

Matthew Sidford, for providing training on the CT3 Texture analyser

Lastly, I would like to thank my family and friends — including my CHEMMAT peers — for providing continuous emotional support and encouragement throughout my final year of engineering.

Contents

Abstract iii

Acknowledgements v

1 Introduction 1
- 1.1 General . . . 1
- 1.2 Project Objectives . . . 2

2 Literature Review/Background 3
- 2.1 General Properties of a Kiwifruit . . . 3
- 2.2 Biological markers of fruit ripeness . . . 3
- 2.3 Background of Non-Destructive Methods for Fruit Ripeness Determination . . . 4
- 2.4 Agarose Potential for Kiwifruit Mimicry . . . 5
- 2.5 Gelation Mechanism of Agarose . . . 5
- 2.6 Tuning the Viscoelastic Properties of Agarose Hydrogels . . . 6

3 Experimental Procedure 11
- 3.1 Hydrogel Sample Preparation . . . 11
  - 3.1.1 Varying Agarose Concentration . . . 11
  - 3.1.2 Varying Soluble Solids Concentration (ssC) . . . 11
  - 3.1.3 Varying Sample Thickness . . . 12
- 3.2 Radio Wave Analysis . . . 13
- 3.3 Texture Analysis . . . 14
  - 3.3.1 Elastic Modulus Determination . . . 15

4 Results and Discussion 17
- 4.1 Texture Analysis . . . 17
  - 4.1.1 Varying Agarose Concentration . . . 17
  - 4.1.2 Varying Soluble Solids Concentration (ssC) . . . 18
  - 4.1.3 Varying Sample Thickness . . . 19
  - 4.1.4 Limitations of Texture Analysis Results . . . 19
- 4.2 Radio Wave Analysis . . . 20
  - 4.2.1 CST Microwave Studio Simulation . . . 21
  - 4.2.2 Varying Agarose concentration . . . 22
  - 4.2.3 Varying Soluble Solids Concentration (ssC) . . . 23
  - 4.2.4 Varying Sample Thickness . . . 24

4.2.5 Limitations of Radio Wave Analysis Results 24
4.3 Correlation Between Reflection Coefficient and Elastic Modulus 26

5 Recommendations for Future Work **27**

6 Conclusions **29**

Bibliography **31**

7 Appendices **35**
7.1 Summary of Collected Data 35
7.2 Safety 36
7.2.1 Material Safety Data Sheets 36

List of Figures

2.1 Kiwifruit anatomy . . . 3
2.2 Fundamental unit of Agarose [23] . . . 5
2.3 Illustration of the two-step agarose gelation process: (a) initial coil to helix transformation (b) helix aggregation [27]" . . . 6
2.4 Graph of ordering temperature against the agarose concentration. Open circle markers represent to High viscosity agarose and solid squares represent Low viscosity agarose. C* represents the critical concentration for chain entanglement in polymer [23] . . . 7
2.5 "Modulus vs Agarose Concentration [28] . . . 7
2.6 "Modulus vs Agarose Concentration [29] . . . 7
2.7 Schematic of gelation with agarose and sugar [24] . . . 8
2.8 Graphs showing the average modulus of a 1 wt% agarose hydrogel with varying sugar concentrations plotted as dark squares: (A) refers to fructose (B) refers to sucrose [24]. Open triangles represent gels with the addition of xanthan gum (not considered in this project) . . . 9

3.1 VNA . . . 13
3.2 S11 vs Frequency plot of 2 wt% agarose hydrogel (Trial 1) . . . 14
3.3 Equipment setup: (1) CT3 Texture Analyser, (2) conical probe and (3) hydrogel sample . . . 14
3.4 Load vs distance graph of a 25 ssC wt% hydrogel (Trial 1) . . . 15
3.5 Load vs surface area graph of a 2 wt% agarose hydrogel (trial 1) - most prominent region (3) was used for elastic modulus calculation . . . 16
3.6 Load vs surface area graph of a 5 wt% ssC hydrogel (trial 1) where a general linear line was fitted for elastic modulus calculation . . . 16

4.1 Experimental results showing changes in elastic modulus with varying agarose concentrations (No fitted regression line due to sparse data) . . . 17
4.2 Experimental results showing changes in elastic modulus with varying ssC (R^2 value = 0.6513) . . . 18
4.3 Comparison of elastic modulus trends (Left: Varying agarose concentration, Right: Varying ssC) . . . 19
4.4 Experimental results showing changes in elastic modulus with varying sample thickness (R^2 value = 0.5791) . . . 20

4.5 Simulated S11 response of micro-strip patch antenna with varying water concentration . . . 21
4.6 Simulated S11 response of micro-strip patch antenna with varying sample thickness for 100 100 wt% water . . . 21
4.7 Experimental results showing changes in S11 with varying agarose concentrations (Red open marker indicates no repeated measurement) . . . 22
4.8 Experimental results showing changes in S11 with varying ssC (R^2 - value = 0.8738) 23
4.9 Comparison of experimental and simulation results of study with varying ssC (Blue Circle: experimental, Orange triangle: simulation) . . . 23
4.10 Experimental results showing changes in S11 with varying sample thickness (R^2 value = 0.2032) . . . 24
4.11 Correlations between S11 and elastic modulus for the following parameters: **(1)** varying agarose concentration (No regression line due to sparse data), **(2)** varying ssC (R^2 value = 0.7414) and **(3)** varying sample thickness (R^2- value =0.4366) 26

7.1 Summary of collected data from Texture and RF analyses . . . 35

List of Tables

3.1 Agarose concentrations studied 12
3.2 Soluble Solids Concentration (ssC) studied 12
3.3 Hydrogel thicknesses studied 13

Chapter 1

Introduction

1.1 General

The kiwifruit industry is New Zealand's largest horticultural sector, with an export value of 1.7 billion NZD in the year 2016 [1]. This export value is predicted to grow to approximately 2.1 billion NZD by 2020 [2]; thus, a large emphasis must be placed on ensuring consistent quality within exported produce. Approximately 20% of exported kiwifruit is measured for ripeness. This is equivalent to 60 million kiwifruit per annum. Current industry methods, such as the *Magness-Taylor Puncture Test*, use firmness as a guideline parameter for kiwifruit ripeness measurement [3]. These destructive measurement methods are proven to be unsustainable, disabling further usage of the fruit and consequently contributing to New Zealand's food wastage statistics.

Considering the fact that individual kiwifruit ripen at different rates [4, 5], testing a small population of kiwifruit does not provide enough accuracy. Moreover, further handling of the produce is carried out after harvest and prior to consumer consumption. This results in a larger degree of uncertainty with produce quality during shipping and handling. Alternative, non-destructive methods must therefore be explored; to minimise the export of poor-quality fruit and reduce food wastage contributed by destructive testing methods.

Previous work has explored the potential of using acoustic signals in order to measure the elastic modulus of kiwifruit [6]. Acoustic waves have demonstrated sensitivity to the interface between hydrogels of different moduli [7]; however, the signals were too noisy to quantify biologically relevant differences in the elastic moduli or free-water content of two kiwifruit models. Other promising non-destructive methods, such as Hyperspectral Imaging and Laser Doppler Vibrometry (LDV), were deemed economically infeasible for industrial applications [8, 9]. Thus, other non-intrusive methods are explored.

Radio-frequency (RF) waves is a novel approach to fruit ripeness testing. RF waves have an increased sensitivity to dielectric properties [10]; thus, the RF spectrum exhibits potential use in detecting free water content in kiwifruit upon ripening. This project aims to validate the use of RF waves as a potential, non-destructive method of measuring kiwifruit ripeness.

The success of the RF sensing device has immense potential in large scale industrial applications, particularly in the Food Industry. Further developments of the sensing technology could provide quality control solutions for a wide range of manufacturing companies; increasing efficiency and reducing food waste. Ultimately, the goal of the project is to integrate flexible, low-cost sensors into cardboard crates where kiwifruit is stored when transported.

1.2 Project Objectives

The main objective of this specific area of research is to refine synthetic testing models which imitate the viscoelastic and dialectic properties of kiwifruit. These models will be used to calibrate micro-strip antennas manufactured by the Electrical and Electronic Engineering department.

In particular, the project aims to:

- Establish specific parameters which affect the viscoelastic and dielectric properties of hydrogels
- Determine hydrogel compositions which mimic kiwifruit flesh during various ripening stages
- Validate the simulated RF data of the micro-strip patch antennas
- Examine correlations between viscoelastic and dielectric properties of hydrogel samples

The high-degree of complexity within the kiwifruit structure is the underlying reason for the use of synthetic models in this project. Parameters such as structure, composition and geometry are convoluted into the final RF signal, creating difficulties in reading RF output signals during calibration. Using controlled materials, such as hydrogels, allow the determination of specific parameters which affect RF output signals.

Chapter 2

Literature Review/Background

2.1 General Properties of a Kiwifruit

Though there are a variety of kiwifruit types, the majority of research available is of the cultivar "Hayward", due to its commercial availability [3, 11].

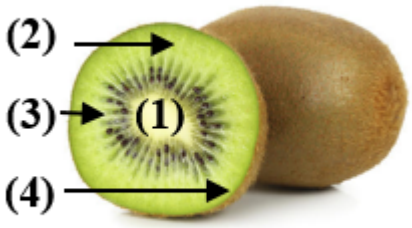

FIGURE 2.1: Kiwifruit anatomy

As shown in Figure 2.1, there are four main tissue zones make up the anatomy of the kiwifruit: (1) the core, (2) the outer pericarp, (3) the inner pericarp, and (4) the skin [3]. Each of these four regions differ in chemical and consequently, mechanical properties [3, 6]. Previous studies confirm that that firmness is highest in the core, followed by the outer pericarp, while the inner pericarp is shown to be the softest and least dense region.

Mechanical and chemical properties are of great importance when determining product quality [12, 13]. Destructive methods, such as the *Magness-Taylor Puncture Test*, are heavily used in industry to test for kiwifruit ripeness, [3, 11–13]. These destructive measurement typically methods obtain the maximum force needed to penetrate the fruit at a certain depth. According to previous studies, a dramatic change in firmness is observed during the ripening stages of kiwifruit.

2.2 Biological markers of fruit ripeness

Significant changes in chemical composition and mechanical properties are a result of the different ripening stages of kiwifruit [4, 14, 15]. As the kiwifruit ripens, the firmness decreases dramatically; a substantial weight loss is also observed throughout the ripening stages [4, 11]. This could be attributed to the decrease in bound water, and consequential increase in free water content. Two distinct ripening stages has been observed from previous studies [3, 14]. This

decrease in firmness is attributed to a decrease in flesh cell adhesion found in the initial stages of ripening. Further loss in cell adhesion and changes in cell wall composition are observed in the later stages of ripening. These studies indicate that kiwifruit texture is highly dependent on the flesh cell adhesion and cell wall composition; results from Harker et al. show that larger cells are found to have more structural integrity [11].

The study has also aimed to correlate relationships between kiwifruit soluble solids concentration (ssC) — which range from 8 – 15 wt% — and fruit firmness [11]. The results of these studies showed inconsistencies which were attributed to slight methodological problems. This study, however, poses the potential of correlating the chemical composition of kiwifruit flesh with changes in firmness properties during ripening. The kiwifruit structure is very complex; thus, certain physical and chemical parameters attributed to ripening must be isolated and analysed in detail. Varying ssC of synthetic testing models could potentially be of use in understanding changes in RF output signal in the presence of sugar-water interactions.

2.3 Background of Non-Destructive Methods for Fruit Ripeness Determination

The movement towards non-destructive methods is induced by the increasing demands of the kiwifruit industry in New Zealand [1]. Food wastage, contributed by destructive methods, must therefore be reduced. Non-invasive and non-destructive ripeness measurement methods demonstrate great potential for research and food industrial applications [7, 16–18]. Numerous studies have looked into non-destructive measuring techniques include the use of Hyperspectral Imaging, Laser Doppler Vibrometer (LDV) and ultrasonic frequency [6, 8, 9]. Hyperspectral Imaging and LDV, however, have been proven to be economically infeasible for large-scale applications [8, 9]. Output signals from the ultrasonic frequency method has displayed great levels of noise in the output signal which makes it an infeasible measurement method despite its lower associated costs [6].

The use of radio frequency (RF) waves is new and novel technique for food industrial applications. Their displayed larger wavelength indicates the potential of overcoming signal noise from over-detecting kiwifruit internal structure — a problem observed in the previous year's study [6]. Studies have displayed the use of RF waves to measure free water content in solutions [10, 19, 20]. The polar nature of water molecules attribute to its strong dielectric properties. RF is sensitive to dielectric properties; thus, changes in kiwifruit free-water content has a consequential effect on the output RF waves. This has been demonstrated with solutions of varying sugar and salt concentrations [10, 19, 20]. Sugar and salt molecules bond with the free-water molecules, reducing the polarisation of the water molecules; this consequently reduces the dielectric constant of the solution.

A Network Analyser and microstrip patch antenna are two common pieces of equipment used together in the analysis of RF waves. The network analyser transports incident RF waves to the

patch antenna; this patch antenna subsequently absorbs or reflects the incident waves depending on the dielectric properties of the sample it is in contact with [10, 19, 20]. Reflected waves are transported back to the Network Analyser, where the following parameters are recorded: (1) reflection co-efficient and (2) frequency of reflected wave [10, 19, 20]. The reflection co-efficient (S11) is a measure of the amount of energy reflected by the antenna. A high S11 magnitude — i.e. more negative S11 values — indicate high amounts of energy delivered to, and reflected by, the patch antenna. The resonance frequency, in these studies, refers to the particular frequency where maximum energy is delivered to the antenna [10, 19, 20]. Increasing salt and sugar concentrations in a water solution is observed to decrease the reflection co-efficient output values in the Network Analyser. This is attributed to the changes in dielectric properties of the solution.

2.4 Agarose Potential for Kiwifruit Mimicry

Agarose is a linear, bio-polymer food gel derived from marine red algae, known as *Rhodophyceae* [21, 22]. Each unit of agarose contains β-1,3 linked D-galactose and α-1,3 linked 3,6 anhydro-αL-galactose residues, as shown in Figure 2.2. Agarose displays several ideal characteristics which contributes to its use in a wide range of industrial applications [21–24]. These include the ability to accommodate a large capacity of water, low chemical complexity, biocompatability, and mechanical stability [21]. Agar-agar — a widely used food-grade gel — contains agarose which acts as its main gelling agent [24]. Polysaccharides, such as agarose, play an important role in biological tissues with cohesion and physical organisation, as well as retention of water [22]. This combination of favourable properties and extensive history of food and non-food industrial applications makes agarose a favourable choice for modelling natural kiwifruit tissue. Furthermore, a recent study has confirmed a good correlation between the viscoelastic behaviour of kiwifruit and agarose hydrogels [6].

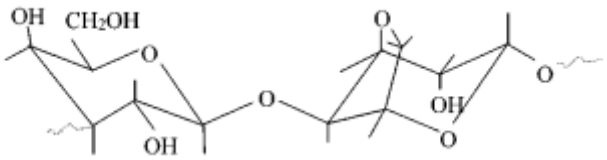

FIGURE 2.2: Fundamental unit of Agarose [23]

2.5 Gelation Mechanism of Agarose

An agarose hydrogel is formed when a homogeneous solution is cooled below the ordering temperature, where the agarose undergoes a coil to helix transformation [23]. Homogeneous solutions are usually formed through the dissolution of agarose in water via heat treatment [22–25]. Specific temperatures for heat treatment and cooling vary depending on the type of

agarose used [22–26]. From previous studies, a temperature range between 70 – 99 °C is required for the dispersal of the gel into solution. A temperature range of 28 – 36 °C is required for gelation; however, it is noted from one study that the ordering temperature is a function of the agarose monomer concentration. This is defined as a cube root relationship with respect to agarose concentration [25]. Figure 2.4 gives an indication of the gelling temperature for different concentrations of agarose at two different viscosities.

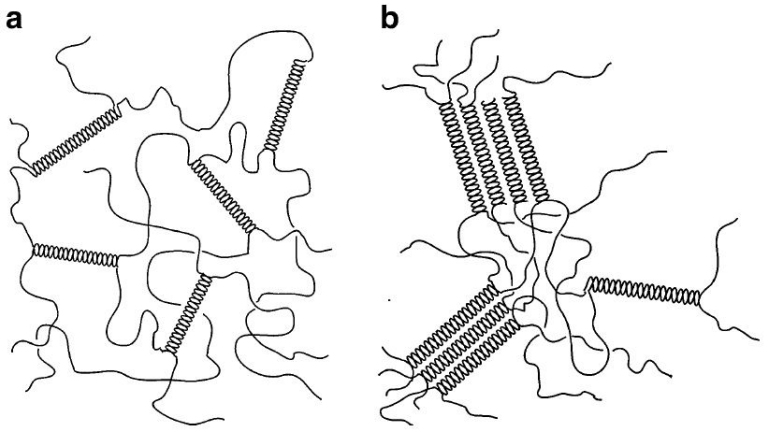

FIGURE 2.3: Illustration of the two-step agarose gelation process: (a) initial coil to helix transformation (b) helix aggregation [27]"

Currently, a full understanding of the precise gelation mechanism of agarose has not yet been achieved; however, several hypotheses with complementary experimental models have been developed over the years [22, 24–26]. The general process of agarose gelation during the cooling stage involves two steps, as illustrated in Figure 2.3. The initial step involves the transformation of agarose coils into double helices that behave as cross-links. The strength of the gel formed in this step is believed to be proportional to the number of double helices formed. Further "hardening" occurs in the second step of gelation, where the double helices aggregate to form a fibrillar crystal network [23, 25, 27]. This helix aggregation is perceived to be the rate-limiting step of the kinetically-controlled gelation process [23]. The transition from solution to gel via cooling is observed to be very quick, producing stable hydrogels [27].

2.6 Tuning the Viscoelastic Properties of Agarose Hydrogels

Several paramaters must be investigated in order to produce agarose hydrogels which accurately mimic the viscoelastic behaviour of kiwifruit. Several studies have assessed the effect of agarose concentration on the bulk elastic modulus of the hydrogel [25, 26, 28, 29]. These studies confirm that an increase in agarose concentration results in a subsequent increase in bulk elastic modulus, as shown in Figures 2.5 and 2.6. The increase in elastic modulus is attributed to the increase in polymer-polymer interactions between the agarose double helices. As a result, stronger and more turbid gels are formed [26].

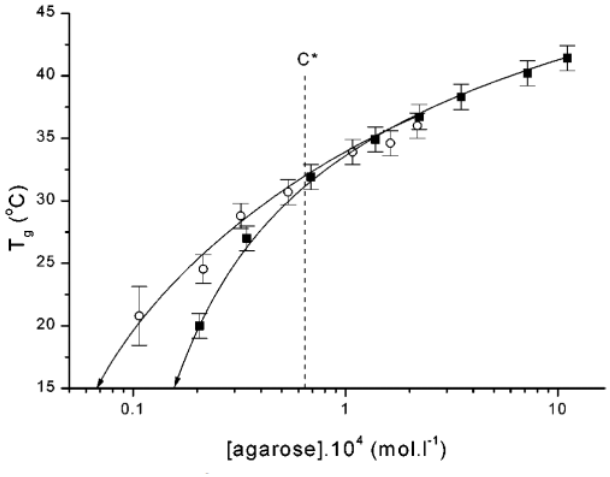

FIGURE 2.4: Graph of ordering temperature against the agarose concentration. Open circle markers represent to High viscosity agarose and solid squares represent Low viscosity agarose. C* represents the critical concentration for chain entanglement in polymer [23]

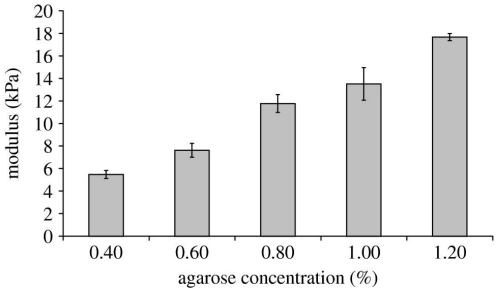

FIGURE 2.5: "Modulus vs Agarose Concentration [28]

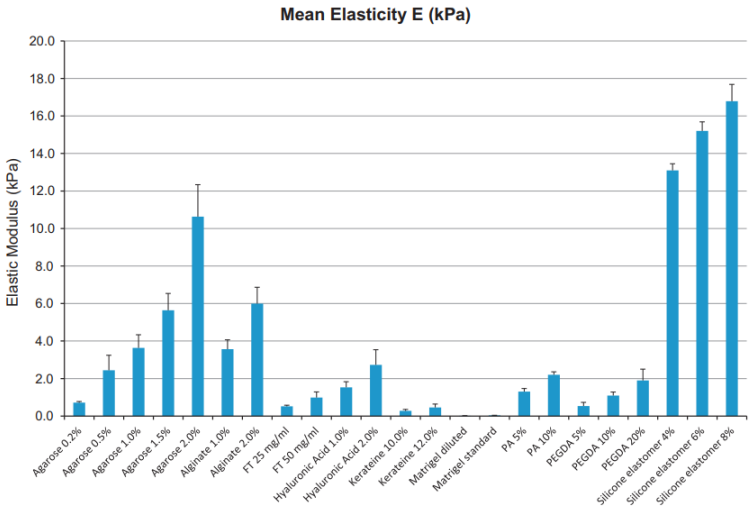

FIGURE 2.6: "Modulus vs Agarose Concentration [29]

Despite the consistency in the relationship of agarose concentration and bulk elastic modulus,

inconsistencies arise in the displayed bulk elastic modulus values of each respective concentration. Yang et al. displays an average bulk elastic modulus of 14 kPa for an agarose concentration of 1 wt%, while studies from Markert et al. — which consider various modulus measurement techniques — obtain an average value of 3.6 kPa for the same agarose concentration [28, 29]. Discrepancies between the two values could potentially be sourced from the methods of agarose preparation and type of agarose powder used for the hydrogels. It has been suggested that thermal history greatly impacts the mechanical and structural properties of the produced hydrogels [30].

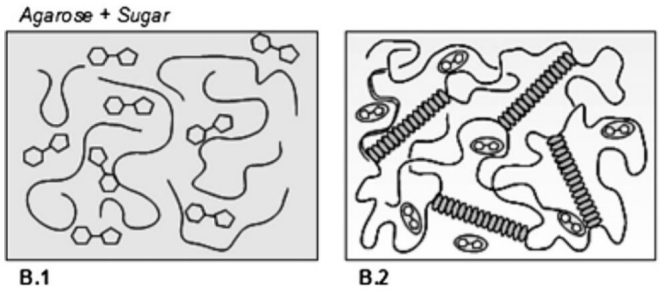

FIGURE 2.7: Schematic of gelation with agarose and sugar [24]

In addition to changes in agarose concentration, the introduction of co-solutes also display considerable effects on the viscoelastic properties of agarose hydrogels. Studies have shown an increase in gel elastic modulus with increasing concentrations of sugar up to a certain extent [24, 31].These studies suggest that the addition of sucrose and glucose advance the formation and aggregation agarose helices, stabilising the cross-links and consequently increasing the strength of the gel network, as shown in Figure 2.8. It is, however, important to note that the excessive addition of sugars result in a contrasting decrease in elastic modulus. Maurer et al. highlights that at sucrose concentrations above 40 wt% display a drastic decrease in elastic modulus of the 1 wt% agarose [24]. The decrease in elastic modulus is proposed to be attributed to the insufficient free water available for creating cross-link zones, due to the surplus of chemical reagents in the solution [31]. This surplus results in a lowered coil to helix transformation, and consequently leads to the structural breakdown of the hydrogel. Moreover, the coil to helix transformation, shown in Figure 2.7 temperature is shifted to lower temperatures. This shift is due to the increase in solvent viscosity with the presence of sugar molecules, resulting in slower gelation dynamics [24].

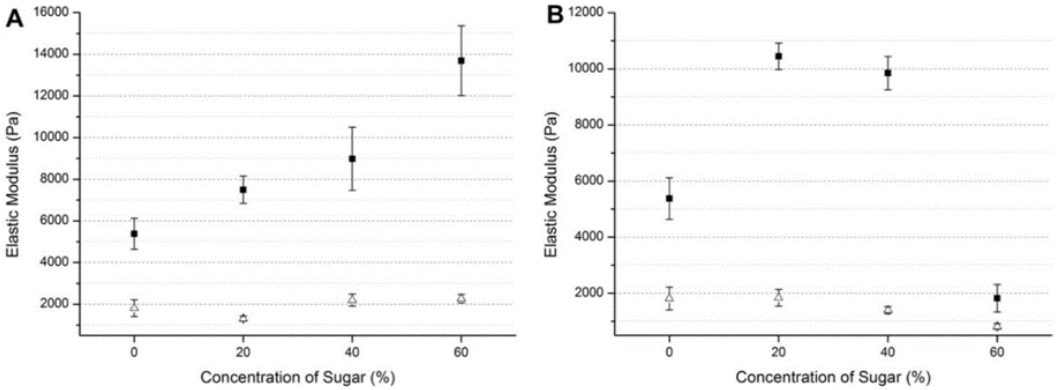

FIGURE 2.8: Graphs showing the average modulus of a 1 wt% agarose hydrogel with varying sugar concentrations plotted as dark squares: (A) refers to fructose (B) refers to sucrose [24]. Open triangles represent gels with the addition of xanthan gum (not considered in this project)

Based on the reviewed literature, variations in agarose and sugars — such as glucose — show potential in further fine-tuning the firmness of the hydrogel testing models. These variations consequently alter the relative water concentration of the hydrogel, which in turn change the RF output signal, as mentioned in Section 2.3.

Chapter 3

Experimental Procedure

3.1 Hydrogel Sample Preparation

Five different hydrogels were created for each of the following three parameters: agarose concentration, glucose concentration and hydrogel thickness.

Materials

- Distilled Water
- Agarose powder
- Glucose powder
- 150 mL beakers
- 85 mm by 38 mm silicon moulds

3.1.1 Varying Agarose Concentration

The initial step for hydrogel sample preparation involved measuring appropriate amounts of agarose and water to produce five 100 g solutions of varying agarose concentrations. Firstly, 1 g of agarose powder and 99 g of distilled water were measured and added in a 150 mL beaker, forming a 1 wt% solution. The beaker was then placed on a hot plate and heated to 99 °C for 30 minutes, or until the powder had dissolved and the solution had transformed into a gel-like consistency. Continuous stirring was provided by the stirring plate and magnetic stirring rod throughout the whole heating process. The mixture was then transferred to the rectangular silicon mould and allowed to cool at room temperature for 1 hour. After setting and cooling, the hydrogel is then refrigerated for 16-24 hours in order to be used the following day. This procedure was repeated for the agarose concentrations, shown in Table 3.1.

3.1.2 Varying Soluble Solids Concentration (ssC)

Appropriate amounts of agarose, glucose and water were initially measured to produce five 50-g solutions of varying soluble solids concentrations. 1.25 g of agarose powder, 1.25 g of glucose

powder and 47.5 g of distilled water were measured and added in a 150 mL beaker, forming a 5 wt% solution. Heating and cooling methods used for this set of hydrogel preparations were similar to that mentioned in Section 3.1.1. This whole procedure was repeated for the soluble solids concentrations, shown in Table 3.2.

3.1.3 Varying Sample Thickness

Hydrogels of different thicknesses were created in order to analyse optimum sample depth for RF data collection. Firstly, 1.5 g of agarose powder and 28.5 g of distilled water were measured and added in a 150 mL beaker, forming a 5 wt% solution. This solution created a 5 mm thick hydrogel. Heating and cooling methods used for this set of hydrogel preparations were similar to that mentioned in Section 3.1.1. This whole procedure was repeated for the hydrogel thicknesses, shown in Table 3.3.

TABLE 3.1: Agarose concentrations studied

Agarose Concentration (wt%)	Amount of Agarose Added (g)	Amount of Water Added (g)
1	1	99
2	2	98
3	3	97
4	4	96
5	5	95

TABLE 3.2: Soluble Solids Concentration (ssC) studied

Soluble Solids Concentration (wt%)	Amount of Agarose Added (g)	Amount of Glucose Added (g)
5	1.25	1.25
10	1.25	3.75
15	1.25	6.25
20	1.25	8.75
25	1.25	11.25

TABLE 3.3: Hydrogel thicknesses studied

Thickness (mm)	Total Weight of Solution (g)	Amount of Agarose Added (g)
5	30	1.5
10	45	2.25
16.5	60	3
26	75	3.75
22	100	5

3.2 Radio Wave Analysis

Materials

- Vector Network Analyser (VNA)
- Coaxial-fed patch antenna
- 8 mm Polystyrene layer
- Hydrogel samples of varying agarose concentration, sugar concentration and thickness
- Hayward kiwifruit

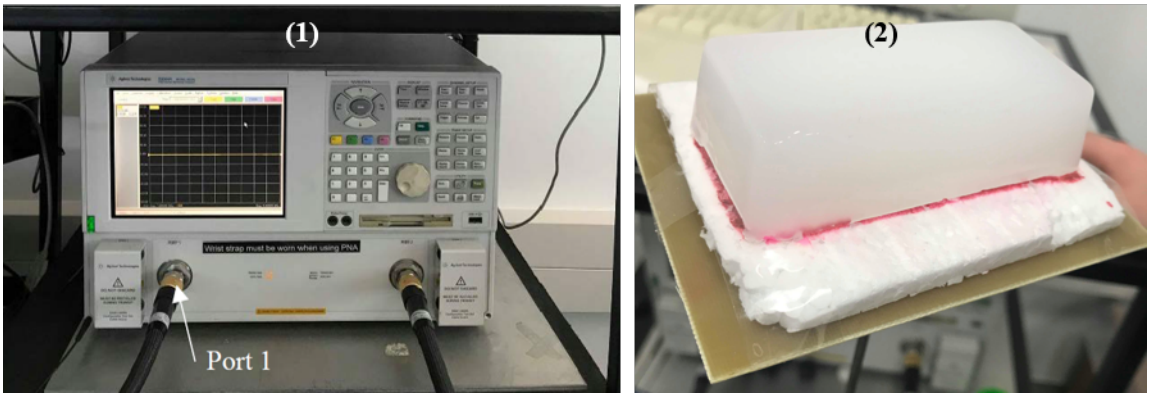

FIGURE 3.1: VNA

Initial equipment set-up and calibration of the VNA and patch antenna shown were performed by fellow 4th year engineering students, Tristan Newhook and Alvin Huang. The polystyrene-covered patch antenna is connected to the VNA via port 1, as shown in Figure 3.1. Each hydrogel was placed on top of the polystyrene layer, ensuring it matches the marked outline. This location enables the hydrogels to cover the entire patch underneath the polystyrene layer and ensures consistency throughout the entire experiment. Data from the patch antenna was automatically transported and displayed as a *S11 vs Frequency (kHz)* graph, exemplified in Figure 3.2, and the relevant S11 value at the resonance frequency was recorded. This procedure was

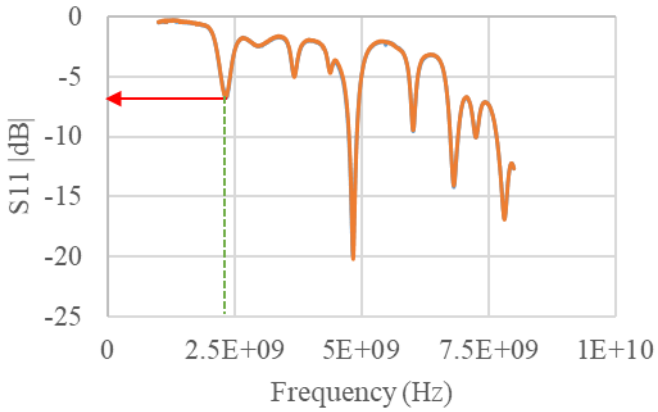

FIGURE 3.2: S11 vs Frequency plot of 2 wt% agarose hydrogel (Trial 1)

repeated once for each hydrogel sample, and the average of the two S11 values were calculated for analysis.

3.3 Texture Analysis

Materials

- CT3 Texture Analyser and complementary software programme (TextureProCT)
- TA2/1000 conical probe, 60°angle
- Hydrogel samples of varying agarose concentration, sugar concentration and thickness
- Hayward Kiwifruit

Gathering hydrogel firmness data involved a series of penetration tests using the CT3 Texture Analyser. The equipment was set up in remote operation, as shown in Figure 3.3, and connected to the appropriate texture analyser software programme via USB Port 4. A normal compression test with a trigger load of 7 g and speed of 0.5 mm/s was undertaken for all samples. It was ensured that the penetrated sections did not overlap and consequently affect the data collected.

FIGURE 3.3: Equipment setup: (1) CT3 Texture Analyser, (2) conical probe and (3) hydrogel sample

A similar method of gathering firmness data was undertaken for kiwifruit. Three different kiwifruits of the same level of ripeness were sliced into 25 mm thick cuts. The core of each kiwifruit underwent the normal compression test with the same load and speed parameters. This procedure was also done for the outer pericarp of each kiwifruit.

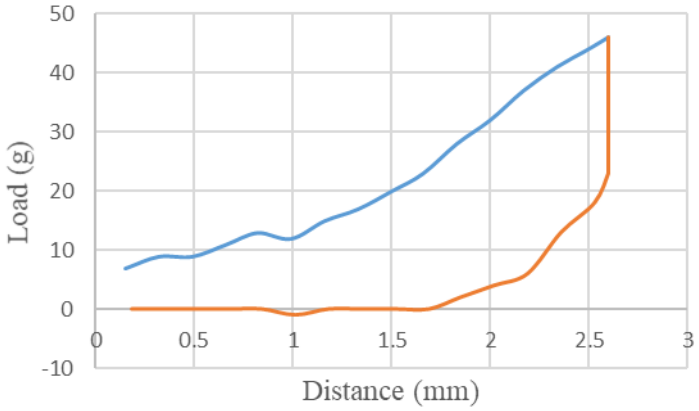

FIGURE 3.4: Load vs distance graph of a 25 ssC wt% hydrogel (Trial 1)

Results from the penetration tests were visually displayed as a *Load (g) vs Distance (mm)* graph, exemplified in Figure 3.4. Numerical data from the series of tests, along with the conical probe dimensions, were used to calculate the elastic modulus, and thus the firmness of the samples.

3.3.1 Elastic Modulus Determination

Microsoft Excel was primarily used for data manipulations. The probe's penetration distance values were converted to equivalent surface area values using Equation 3.1, where h is the displacement of the cone from the trigger load point. The angle of the probe, θ, remains constant at 60 °.

$$SurfaceArea_{cone}(mm^2) = \pi h^2 \frac{tan\frac{\theta}{2}}{cos\frac{\theta}{2}} \tag{3.1}$$

Calculated surface area values were used to re-plot the raw graph into *Load vs Surface Area* graphs, exemplified in Figure 3.5. As shown in the figure, two different linear regions were selected for a particular trial run, and their respective gradients were calculated. This was repeated for all three penetration tests on the same hydrogel. Data was then re-assessed and the final elastic modulus of the 2 wt% agarose hydrogel was determined by calculating the average of only the most prominent linear regions of the three penetration tests.

Due to the oscillating nature of the varying ssC wt% graphs, a general linear trend-line was fitted, as illustrated in Figure 3.6. The elastic modulus was then calculated by taking the average gradient of the three linearly-fitted regions.

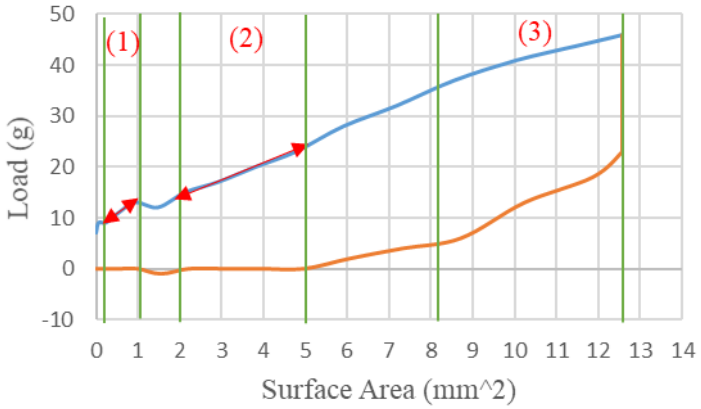

FIGURE 3.5: Load vs surface area graph of a 2 wt% agarose hydrogel (trial 1) - most prominent region (3) was used for elastic modulus calculation

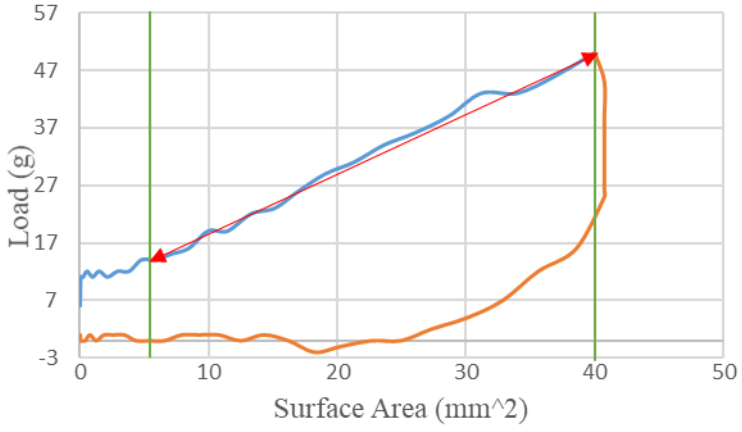

FIGURE 3.6: Load vs surface area graph of a 5 wt% ssC hydrogel (trial 1) where a general linear line was fitted for elastic modulus calculation

Chapter 4

Results and Discussion

4.1 Texture Analysis

The following results are presented as plots of elastic modulus with respect to the three varying parameters studied. A regression model was fitted in each of these graphs to analyse the effects of varying parameters on the overall firmness of the hydrogels. Error bars fitted in the plotted graphs were established through the calculation of standard deviation within the two repeated measurements for each sample.

4.1.1 Varying Agarose Concentration

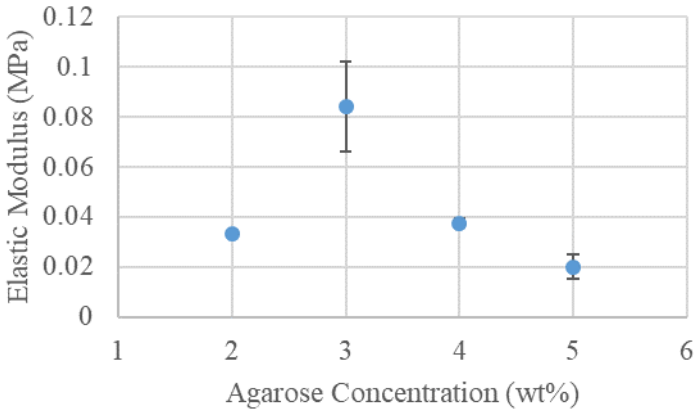

FIGURE 4.1: Experimental results showing changes in elastic modulus with varying agarose concentrations (No fitted regression line due to sparse data)

The results shown in Figure 4.1 indicate a decreasing trend in elastic modulus between concentrations of 3 – 5 wt% agarose. This trend deviates from the expected trend gathered from previous studies, which show that an increase in agarose concentration results in a subsequent increase in elastic modulus. Agarose forms a physical hydrogel which consists of non-covalent, hydrogen bonds. These non-covalent bonds are suggested to fluctuate with change in agarose concentration [27]; thus the observed decrease in elastic modulus could potentially be attributed to the non-covalent bond fluctuations affecting the strength of the gel network.

Discrepancies between the experimental results and predicted trends may also be due to slight inconsistencies with the heating and gelation temperatures of the agarose solutions. As shown in a previous study, thermal history has a huge influence on the overall textural properties of agarose hydrogels [30].

It is important to note several key issues which took place during the hydrogel sample preparation for varying agarose concentrations. Firstly, agarose concentrations of 1 wt% and below did not form a gel. This does not agree with the critical concentration for gelation, shown in Fig 2.4. Critical concentrations for gelation are therefore highly specific to the type of agarose used. From this experiment with *Type I-A, low EEO* agarose, it is concluded that an agarose concentration of at least 2 wt% is required to form a gel. Secondly, agarose concentrations above 10 wt% failed to create smooth, homogeneous gels. Thus, pure agarose gels has a very limited concentration range at which a satisfactory hydrogel can be formed.

4.1.2 Varying Soluble Solids Concentration (ssC)

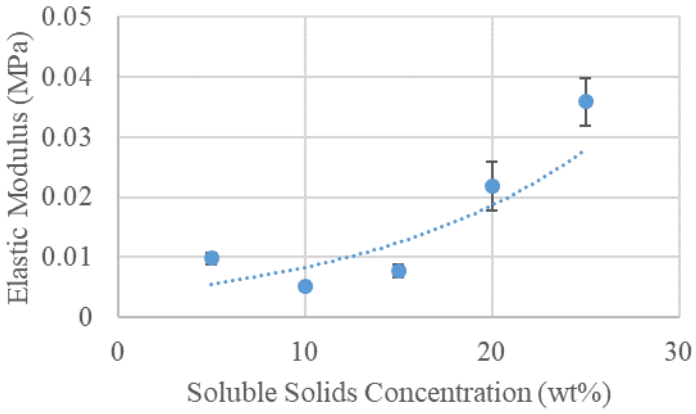

FIGURE 4.2: Experimental results showing changes in elastic modulus with varying ssC (R^2 value = 0.6513)

An increase in elastic modulus with increasing ssC is observed in Figure 4.2. This complies with previous studies which indicate an increase in gel-network connectivity with increasing amounts of sugar [24, 31]. Glucose has been shown to promote coil-to-helix formation and helix aggregations; thus, a greater number of stabilised cross-links are formed which consequently increases the strength of the hydrogel. It is noted that the 5 wt% agarose-glucose hydrogel demonstrates a higher elastic modulus in comparison to the 10 wt% hydrogel. As previously mentioned, this decrease in elastic modulus could be attributed to the fluctuations in the non-covalent interactions of the physical gels with time and temperature. Previous studies have also mentioned sudden decreases in elastic modulus with very high concentrations of sugar; this could potentially limit the application of binary agarose-glucose hydrogels.

The contrasting elastic modulus trends between variation of the two aforementioned parameters are highlighted in Figure 4.3. Differences with elastic modulus values are also observed between the two parameters, which agree with comparisons shown in the study conducted by

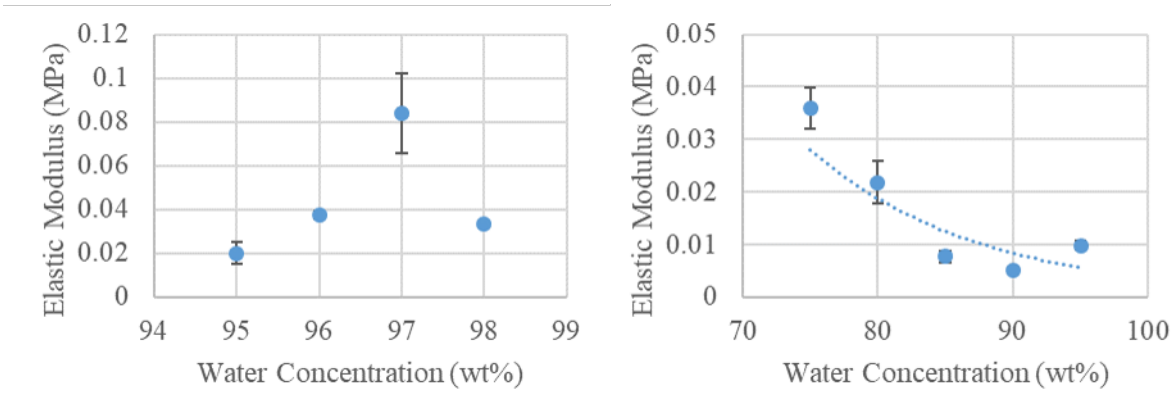

FIGURE 4.3: Comparison of elastic modulus trends (Left: Varying agarose concentration, Right: Varying ssC)

Maurer et al. [24]. From the texture analysis results, 5 wt% pure agarose hydrogels are observed to be two times stiffer than binary hydrogels of the same concentration. Their noted values are 0.020 $\pm$0.0050 MPa and 0.0098 $\pm$0.00093 MPa, respectively. Addition of non-gelling monosaccharides, therefore, exhibit the potential to allow controlled alteration of the viscoelastic properties of agarose hydrogels.

It is also worth noting that binary hydrogels enable a wider range of gels, with respect to water concentration. Binary hydrogels therefore establish a greater potential in being able to calibrate the developed microstrip patch antennas. Furthermore, it is suggested that the addition of sugars prevent the hydrogels from undergoing syneresis. The agarose hydrogels were stored for approximately 48 hours before Texture Analysis took place; liquid inside the gel may have seeped out and affected the subsequent firmness experimental results. This has been a common occurence with pure agarose hydrogels [21]. Previous studies have noted that binary agarose-sugar hydrogels established a higher water-holding capacity which in turn reduces the occurrence of syneresis [24]. This is an ideal property for long-term use of hydrogels.

4.1.3 Varying Sample Thickness

Though the regression line in Figure 4.4 indicates a decreasing elastic modulus with increasing sample thickness, the regression model is statistically insignificant due to the presence of the outlier for a sample thickness of 13 mm. The plotted graph, however, indicates that samples must be at least 15 mm in order to achieve reproducible firmness results. This may be of particular importance when relating to the average physical dimensions of a kiwifruit [3, 4].

4.1.4 Limitations of Texture Analysis Results

As previously mentioned, inaccuracies within the presented data may be attributed to the hydrogels undergoing syneresis and consequently reducing the accuracy of the initial measured concentrations. Furthermore, potential errors may originate form inaccurate elastic modulus

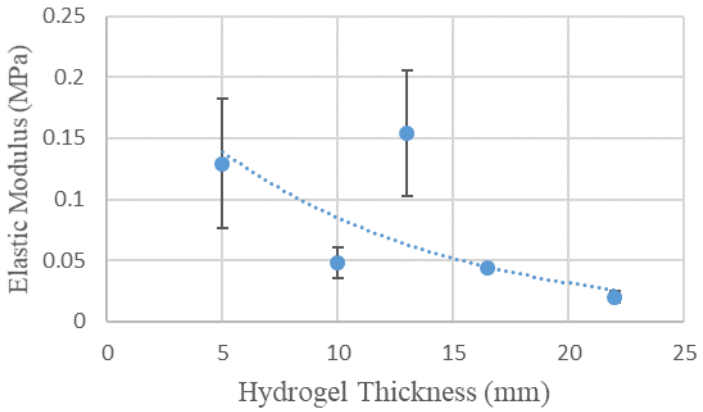

FIGURE 4.4: Experimental results showing changes in elastic modulus with varying sample thickness (R^2 value = 0.5791)

calculations; the calculated best-fit gradient of the *Load (N) vs Surface Area (mm^2)* may not be an accurate representation of the samples' elastic moduli. The level of noise, exemplified in Figure 3.6, increases the difficulty in accurately determining the elastic modulus of each hydrogel. Inhomogeneity may be present in the hydrogel samples which accounts for the noise and errors in elastic modulus calculations. These sources of measurement error were reduced through calculating the average of three repeated measurements for each sample and indication of degrees of uncertainty.

Binary agarose-glucose hydrogels establish the greatest potential for controlled alteration of viscoelastic properties; this of great importance when assessing the potential for kiwifruit mimickry. Texture analyser results show an average kiwifruit core firmness of 0.13 $\pm$0.055 MPa, and an outer pericarp firmness of 0.052 $\pm$0.005 MPa. Discrepancies between kiwifruit results from previous studies are attributed to the variation in kiwifruit cultivar and sourced regions, which have consequential effect on the chemical and mechanical properties of the fruit [3, 4, 6, 11]. A limitation in this study is therefore the lack of reliable information available for firmness measurements of specific types of kiwifruit. Moreover, sourcing kiwifruit of different levels of ripeness has proven to be a challenge. In order for the hydrogels to accurately mimic kiwifruit flesh, sufficient kiwifruit firmness information must be gathered for various stages (i.e. unripe, ripe, overripe). Despite this lack of information, kiwifruit firmness measurements from this study indicate that an increase in glucose is required in binary agarose-glucose hydrogels in order to obtain a higher elastic modulus, similar to that of the analysed kiwifruit.

4.2 Radio Wave Analysis

The following results are presented as plots of S11 values with respect to water concentration and thickness. A regression model was fitted for each of these graphs to analyse the effects of varying parameters on the overall energy absorbency at the 2.45 GHz resonance frequency. Error bars fitted in the plotted graphs were established through the calculation of standard

deviation within the three repeated measurements for each sample. Comparisons between the simulated and experimental data are made using a a standard t-test. The null-hypothesis of this test suggests that there is no difference in the means of the experimental and simulated results.

4.2.1 CST Microwave Studio Simulation

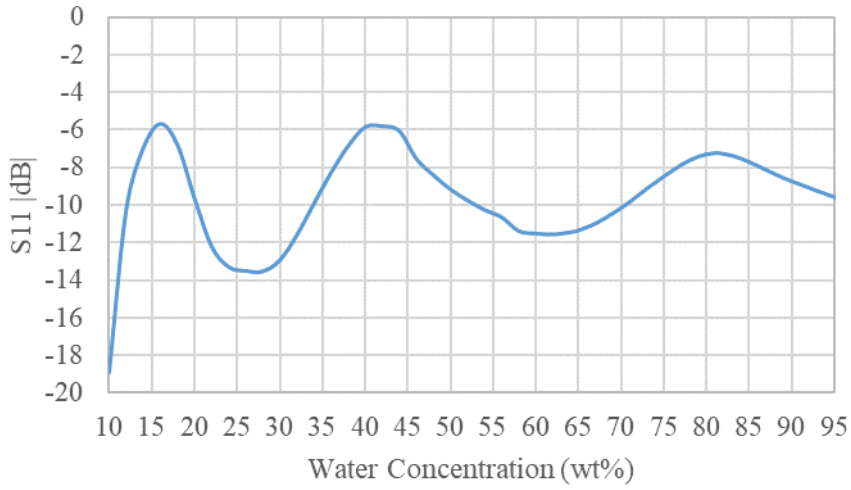

FIGURE 4.5: Simulated S11 response of micro-strip patch antenna with varying water concentration

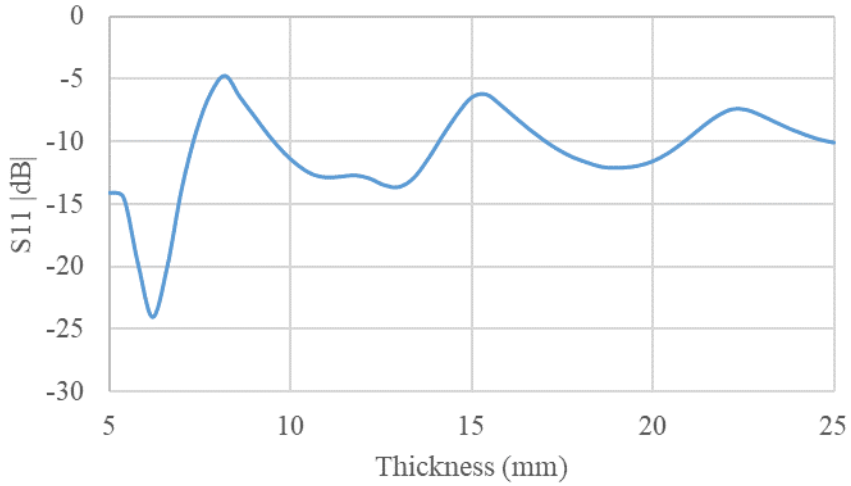

FIGURE 4.6: Simulated S11 response of micro-strip patch antenna with varying sample thickness for 100 100 wt% water

Figures 4.5 and 4.6 show simulations of the designed micro-strip patch antenna via *CST Microwave Studio*. Both simulations exhibit fluctuations in S11 values with respect to varying water concentration and thickness, which differs from the results of previous studies [10, 19, 20]. These simulated oscillations indicate a sample behaviour which is comparable to a *Fabry*

Perot Cavity; the upper and lower surfaces of the sample act as internal reflectors of the incident RF wave [32].

The increase in water concentration results in a subsequent increase in relative permittivity; this consequently decreases the velocity of the incident RF wave and increases the the wavelength, λ. This induces a proportional increase in the electrical thickness, t, of the sample. A similar phenomena can be attributed to the variation of sample thickness in Figure 4.6.

Assuming that the incident RF waves are striking the sample plane perpendicularly, when t is a multiple of $\frac{\lambda}{2}$, minimum reflections occur — this is observed at the plotted troughs with minimum S11 values. Conversely, when t deviates away from a multiple of $\frac{\lambda}{2}$, the RF waves are reflected back to the micro-strip patch antenna; hence, the S11 values increase. Agarose hydrogels of varying water concentrations and thicknesses were used to validate the observed relationship in the simulations presented.

4.2.2 Varying Agarose concentration

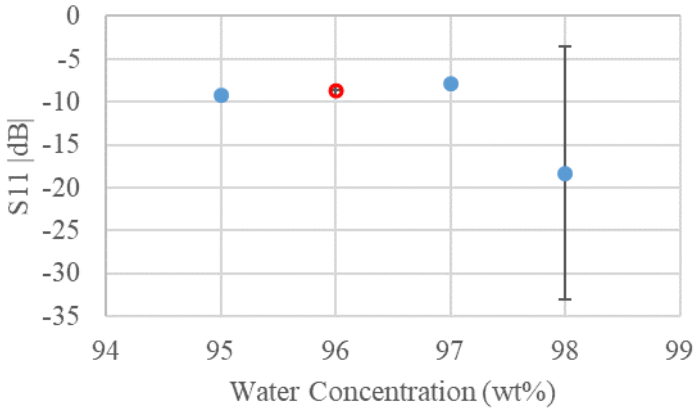

FIGURE 4.7: Experimental results showing changes in S11 with varying agarose concentrations (Red open marker indicates no repeated measurement)

As observed in Figure 4.7, increasing the water concentration from 95 wt% to 97 wt% consequently increases the S11 value. This could be attributed the deviation of t from the $\frac{\lambda}{2}$ multiple. There is a significant degree of uncertainty observed in the 98 wt% water sample which potentially contributes to its deviation away from the aforementioned trend.

Due to the limited data available, a relationship cannot be concluded for this particular study on the effects of agarose concentration. It may be of use to note that the experimental S11 value at 95 wt% water (i.e. 5 wt% agarose) is -9.26 $\pm$0.15 while the simulated S11 value for the same concentration is -9.6. This minute difference in the simulated and experimental value shows promising potential, however, a larger data set is required to for a satisfactory correlation to be established.

4.2.3 Varying Soluble Solids Concentration (ssC)

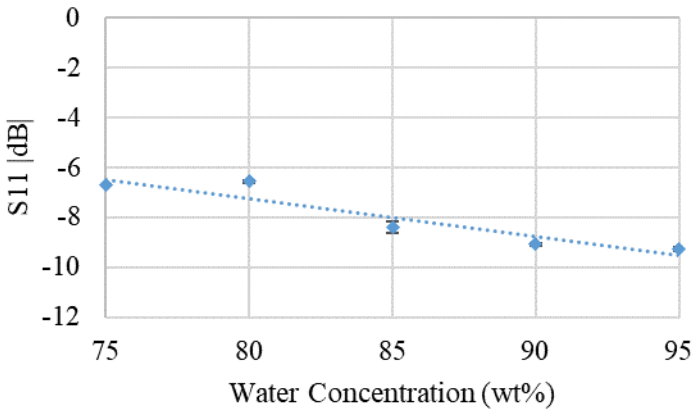

FIGURE 4.8: Experimental results showing changes in S11 with varying ssC (R^2 - value = 0.8738)

There is an observed decrease in S11 with increasing water concentration, as shown in Figure 4.8. This is potentially attributed to*t* increasing moving towards a multiple value of $\frac{\lambda}{2}$. The results show a minimal degree of uncertainty; this indicates satisfactory S11 reproducibility with binary agarose-glucose hydrogels. S11 results from binary agarose-glucose hydrogels obtain a similar trend with the simulation, shown in Figure 4.5

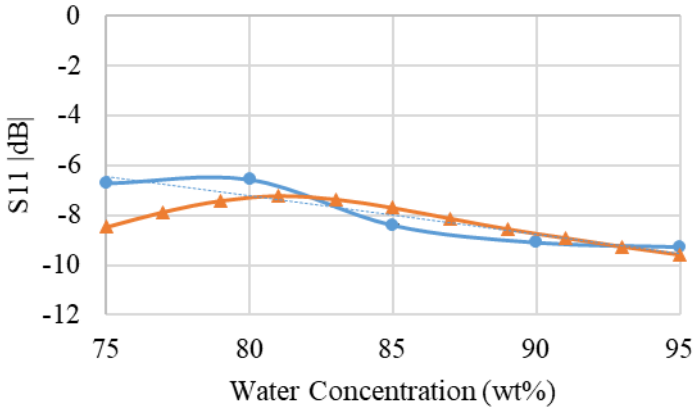

FIGURE 4.9: Comparison of experimental and simulation results of study with varying ssC (Blue Circle: experimental, Orange triangle: simulation)

The predicted profile exhibits a slight shift in the maximum S11 value, which is attributed to to external factors. The simulated results from *CST Microwave Studio* did not account for broadening effects, such as water content in the atmosphere and slight thickness variations in the polystyrene *"air gap"* layer. Despite observed discrepancies within the two sets of data, a t-test output p-value of 0.3 is obtained (i.e. value greater than $\alpha = 0.05$); thus, the null-hypothesis cannot be neglected. Binary agarose-glucose hydrogels, therefore, show great potential in calibrating the Network Analyser and micro-strip patch antennas for ripeness assessment via measurement of free-water concentration.

4.2.4 Varying Sample Thickness

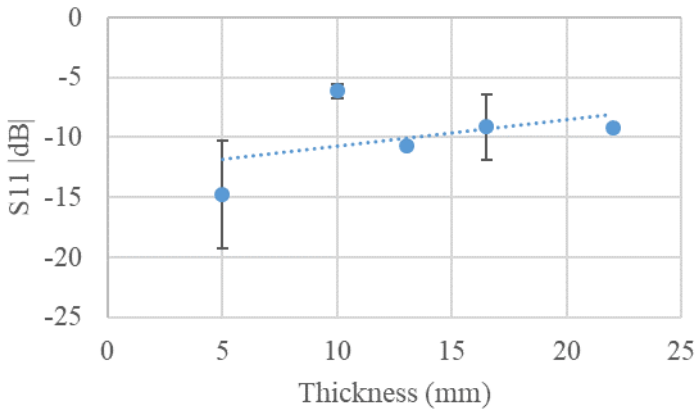

FIGURE 4.10: Experimental results showing changes in S11 with varying sample thickness (R^2 value = 0.2032)

Significant degrees of uncertainty are observed in 5 mm and 16.5 mm agarose hydrogel samples, as shown in Figure 4.10. The regression model fitted states that for this range of thicknesses, an increase in thickness causes an increase in S11 value; it is, however, important to note the low R^2 value associated with the regression line. There is no observed statistically significant relationship between S11 and thickness. The simulated results for varying thickness establish a fluctuating relationship, with a high degree of complexity relating to the physical model; it is therefore necessary to validate these simulated results with experimental results. However, the simulation produced was specific to samples of 100 wt%; thus, disabling the possibility of data validation.

4.2.5 Limitations of Radio Wave Analysis Results

Discrepancies between experimental and theoretical results are attributed to inaccuracies in hydrogel concentration measurements due to uncontrolled expulsion of liquid from the gel, as detailed previously in Section 4.1.4. Again, this source of error is reduce by repeating RF measurements, calculating the average S11 value and deviation the standard deviation of all trials for each sample.

Limitations to the wider aim of this project include the physical dimensions of the agarose hydrogels. The observed deviation of experimental results from simulated data, shown in Figure 4.9, suggest that the incident RF waves do not strike the hydrogel samples perpendicularly; thus, shifting the positions of the S11 peaks and troughs. As the micro-strip antennas required gel samples which cover the entire patch, hydrogel samples created were large and rectangular. This difference in contact surface area between the antenna and sample presents a higher degree of complexity when dealing with real, round kiwifruit samples with no flat surfaces. Moreover, the lack of S11 data for real kiwifruit at different ripeness stages — and therefore

different water concentrations — limits the potential of binary agarose-glucose hydrogels as a choice for kiwifruit flesh mimicry.

It is important to note the associated cost of the VNA and the equipment configuration for S11 measurement. The VNA is a very expensive piece of equipment; it is therefore economically infeasible to use the VNA for large-scale industrial applications. Furthermore, the developed micro-strip patch antenna — though it is small and light — requires constant connection with the VNA; this limits the implementation of antennas on kiwifruit crates.

4.3 Correlation Between Reflection Coefficient and Elastic Modulus

There is no statistically significant correlation between S11 and elastic modulus, as observed in Figure 4.11. A simple linear regression fit was used for the plotted data; this does not provide a satisfactory R^2 value for establishing the relationship between the two parameters. It is, therefore, recommended to solely focus on S11 changes when examining each of the three parameters studied. Conversely, a possible relationship between S11 and elastic modulus through the use of a different analytic method.

Despite the lack of statistically significant correlations between elastic modulus and S11, binary agarose-glucose hydrogels show promising results in obtaining expected viscoelastic response and S11 output values. However, further research on fine-tuning hydrogels is required to successfully calibrate micro-strip patch antennas for kiwifruit ripeness determination.

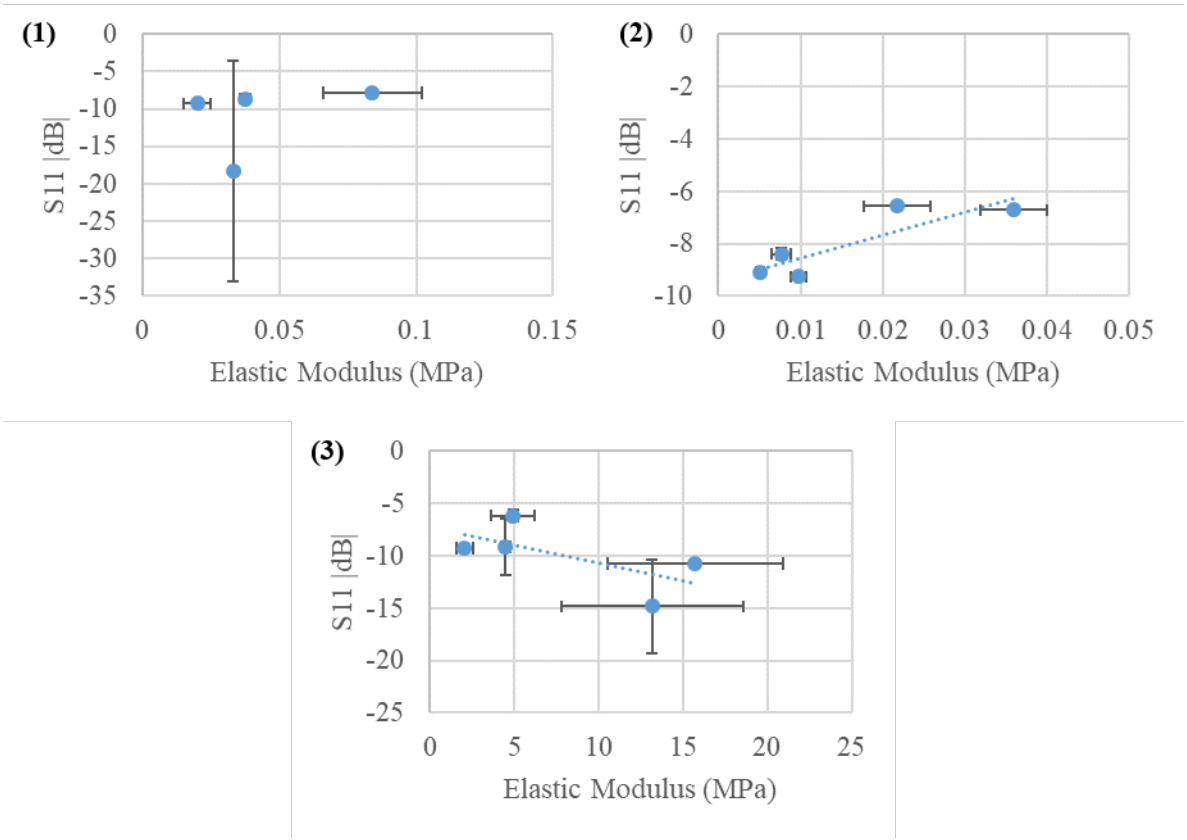

FIGURE 4.11: Correlations between S11 and elastic modulus for the following parameters: **(1)** varying agarose concentration (No regression line due to sparse data), **(2)** varying ssC (R^2 value = 0.7414) and **(3)** varying sample thickness (R^2-value =0.4366)

Chapter 5

Recommendations for Future Work

Limitations highlighted in Sections 4.1.4 and 4.2.5 enable the identification of areas for further research and experimental improvements. In order to properly assess the accuracy of the agarose hydrogels in kiwifruit mimicry, an updated kiwifruit database must be created to breakdown the complexity of the kiwifruit structure. The database must contain viscoelastic and dielectric kiwifruit properties which are categorised by cultivar and origin. It is, therefore, necessary to carry out RF measurements for kiwifruit of varying types and stages of ripeness. Determination of different levels of ripeness may require the initial destructive testing of kiwifruit; the unharmed kiwifruit from the same batch can be used for RF analysis.

Further developments in hydrogel sample preparation techniques are needed for accurate fine-tuning of viscoelastic properties and output S11 values. Moisture loss during preparation and storage times, therefore, need to be quantitatively examined and reduced. As binary agarose-glucose hydrogels have shown an improved water-holding capacity in comparison to pure agarose hydrogels, it is recommended that future research focuses on this specific hydrogel. Analysis of a wider range of ssC is necessary to understand the effects of increasing glucose amounts in the agarose hydrogel. This will enable a consequently wider water concentration range which can be used to further validate the S11 values from *CST Microwave Studio* simulations.

In addition to hydrogel sample improvements, further developments in micro-strip patch antennas and complementary simulations must take place. External factors such as atmospheric water content, variations in sample contact must be considered throughout the developmental stages of the micro-strip patch antennas. As previously mentioned, the observed *Fabry Perot Cavity* phenomena must be further validation with a wider range of hydrogels and real kiwifruit at varying ripeness stages.

The future aim of this project is to implement these micro-strip antennas on kiwifruit crates for on-line monitoring of kiwifruit quality. It is therefore necessary to develop an antenna design which is capable of being printed on cardboard crates. Further research must investigate designs for more robust, flexible antennas with complementary signal processing techniques which accommodate online sensing applications throughout the kiwifruit lifespan — from harvest to consumption.

Chapter 6

Conclusions

The kiwifruit industry has a significant contribution to New Zealand's economy; thus, maintenance of produce quality is of utmost importance. Radio-frequency (RF) waves analysis shows great promise in non-destructively determining the ripeness of kiwifruit throughout its lifespan – from harvest to consumption.

Synthetic, agarose hydrogels of varying concentrations and thicknesses were created to to validate the use of RF waves as a potential, non-destructive method of measuring kiwifruit ripeness. This was achieved through S11 measurements using the developed microstrip patch antenna and Vector Network Analyser (VNA). Texture analysis was also carried out in order to gain insight on the hydrogels' respective firmness values. Sources of errors throughout these analyses were reduced through repeated trials and calculations of degrees of uncertainty. Several conclusions are drawn out from this study:

- Binary agarose-glucose hydrogels demonstrate the greatest potential for fine-tuning specific viscoelastic and dielectric properties
- Pure agarose hydrogel are two times stiffer than binary agarose-glucose hydrogels, with values of 0.020 $\pm$0.0050 MPa and 0.0098 $\pm$0.00093 MPa, respectively
- Non-covalent, hydrogen bond fluctuations within the gel network attribute to the discrepancies of experimental results with the expected theoretical trend
- Simulations from the *CST Microwave Studio* indicate a sample behaviour comparable to a Fabry Perot Cavity — these acount for the observed fluctuations in S11 values with respect to water concentration and thickness
- Comparisons between the simulated S11 data and experimental results with binary hydrogels obtain a p-value of 0.3 — the null-hypothesis, therefore, cannot be neglected
- No statistically significant correlation is established between elastic modulus (viscoelastic property) and S11 output value (dielectric property)

This initial success of free-water content measurement using microstrip patch antennas demonstrate the potential for non-destructive measurement methods to be implemented in the ever-growing kiwifruit industry.

Bibliography

[1] The New Zealand Horticutural Export Authority, Ed. (2016). Kiwifruit industry profile.

[2] Ministry of Primary Industries, Ed. (2018). Situation and outlook for primary industries data.

[3] S. Razavi and M. Bahram-Parvar, "Some physical and mechanical properties of kiwifruit", vol. 3, pp. 1–16, Jan. 2007.

[4] R. Tabatabaekoloor, "FOCUS: Bio-mechanical behavior of kiwifruit as affected by fruit orientation and storage conditions", Sari Agricultural Sciences and Natural Resources University, Jul. 2014, pp. 1–8.

[5] J. Burdon, D. McLeod, N. Lallu, J. Gamble, M. Petley, and A. Gunson, "Consumer evaluation of "hayward" kiwifruit of different at-harvest dry matter contents", *Postharvest Biology and Technology*, vol. 34, no. 3, pp. 245–255, 2004, ISSN: 0925-5214. DOI: 10.1016/j.postharvbio.2004.04.009.

[6] N. Mamidi, "Calibrating an acoustic ripeness tester for kiwifruit", University of Auckland, Department of Chemical and Materials engineering, Tech. Rep., 2017.

[7] "Maturity effects on dielectric properties of apples from 10 to 4500 mhz", *LWT - Food Science and Technology*, vol. 44, no. 1, pp. 224–230, 2011, ISSN: 0023-6438. DOI: https://doi.org/10.1016/j.lwt.2010.05.032.

[8] S. Serranti, G. Bonifazi, and V. Luciani, "Non-destructive quality control of kiwi fruits by hyperspectral imaging", 2017. DOI: 10.1117/12.2255055.

[9] Z. Oveisi, S. Minaee, S. Rafiee, A. Eyvani, and A. Borghei, "Application of vibration response technique for the firmness evaluation of pear fruit during storage", vol. 51, Nov. 2012.

[10] E. M. Cheng, M. Fareq, S. A. B., Y. S. L. Mohd Afendi R., S. F. Khor, W. H. Tan, N. F. M. N., A. Z. Abdullah, and M. A. Jusoh, "Development of microstrip patch antenna sensing system for salinity and sugar detection in waterapplication of vibration response technique for the firmness evaluation of pear fruit during storage", *International Journal of Mechanical & Mechatronics Engineering*, vol. 14, no. 5, pp. 31–36, Oct. 2014.

[11] F. Harker and I. Hallett, "Physiological and mechanical properties of kiwifruit tissue associated with texture change during cool storage", *Journal of the American Society for Horticultural Science*, vol. 119, no. 5, pp. 987–993, 1994.

[12] E. Costell, A. Tárrega, and S. Bayarri, "Food acceptance: The role of consumer perception and attitudes", *Chemosensory Perception*, vol. 3, no. 1, pp. 42–50, Mar. 2010. DOI: 10.1007/s12078-009-9057-1.

[13] M. Larijani, M. Salar, and H. Kargarpour, "Mechanical analysis kiwi's texture and skin using texture analyzer set",

[14] P. A. McAtee, A. C. Richardson, N. J. Nieuwenhuizen, K. Gunaseelan, L. Hoong, X. Chen, R. G. Atkinson, J. N. Burdon, K. M. David, and R. J. SchafferEmail, "The hybrid non-ethylene and ethylene ripening response in kiwifruit (actinidia chinensis) is associated with differential regulation of mads-box transcription factors", *BMC Plant Biology*, vol. 15, no. 1, pp. 1–16, 2015. DOI: 10.1186/s12870-015-0697-9.

[15] N. Simona, G. Joanna, A. L. G, W. M. W, C. M. J, F. Jinquan, and H. F. Roger, "Dry matter content and fruit size affect flavour and texture of novel actinidia deliciosa genotypes", *Journal of the Science of Food and Agriculture*, vol. 91, no. 4, pp. 742–748, DOI: 10.1002/jsfa.4245.

[16] N. Jamal, Y. Yi-bin, W. Jian-ping, R. Xiu-qin, and Y. Chao-gang, "Firmness evaluation of melon using its vibration characteristic and finite element analysis", *Journal of Zhejiang University Science B*, vol. 6, no. 6, pp. 483–490, 2005. DOI: 10.1631/jzus.2005.B0483.

[17] P. Yoiyod and M. Krairiksh, "Analysis of a cost-effective remote sensing system for fruit monitoring", in *2013 IEEE Antennas and Propagation Society International Symposium (APSURSI)*, Jul. 2013, pp. 1086–1087. DOI: 10.1109/APS.2013.6711203.

[18] O. Sipahioglu and S. Barringer, "Dielectric properties of vegetables and fruits as a function of temperature, ash, and moisture content", *Journal of Food Science*, vol. 68, no. 1, pp. 234–239, DOI: 10.1111/j.1365-2621.2003.tb14145.x.

[19] R. Garg, P. Bhartia, I. J. Bahl, and A. Ittipiboon, *Microstrip antenna design handbook*. Artech house, 2001, ch. 4, pp. 291–292.

[20] M. T. Islam, M. N. Rahman, M. S. J. Singh, and M. Samsuzzaman, "Detection of salt and sugar contents in water on the basis of dielectric properties using microstrip antenna-based sensor", *IEEE Access*, vol. 6, pp. 4118–4126, 2018, ISSN: 2169-3536. DOI: 10.1109/ACCESS.2017.2787689.

[21] R. Imani, S. H. Emami, P. R. Moshtagh, N. Baheiraei, and A. M. Sharifi, "Preparation and characterization of agarose-gelatin blend hydrogels as a cell encapsulation matrix: An in-vitro study", *Journal of Macromolecular Science, Part B*, vol. 51, no. 8, pp. 1606–1616, 2012. DOI: 10.1080/00222348.2012.657110.

[22] M. Tako and S. Nakamura, "Gelation mechanism of agarose", *Carbohydrate Research*, vol. 180, no. 2, pp. 277–284, 1988, ISSN: 0008-6215. DOI: https://doi.org/10.1016/0008-6215(88)80084-3.

[23] V. Normand, D. L. Lootens, E. Amici, K. P. Plucknett, and P. Aymard, "New insight into agarose gel mechanical properties", *Biomacromolecules*, vol. 1, no. 4, pp. 730–738, 2000. DOI: 10.1021/bm005583j.

[24] S. Maurer, A. Junghans, and T. A. Vilgis, "Impact of xanthan gum, sucrose and fructose on the viscoelastic properties of agarose hydrogels", *Food Hydrocolloids*, vol. 29, no. 2, pp. 298–307, 2012, ISSN: 0268-005X. DOI: https://doi.org/10.1016/j.foodhyd.2012.03.002.

[25] M. R. Letherby and D. A. Young, "The gelation of agarose", *Journal of the Chemical Society, Faraday Transactions 1: Physical Chemistry in Condensed Phases*, vol. 77, no. 12, pp. 1953–1966, 1981. DOI: https://doi.org/10.1039/F19817701953.

[26] L. M. Barrangou, C. R. Daubert, and E. A. Foegeding, "Textural properties of agarose gels. i. rheological and fracture properties", *Food Hydrocolloids*, vol. 20, no. 2, pp. 184–195, 2006, 7th International Hydrocolloids Conference, ISSN: 0268-005X.

[27] D. Nordqvist and T. A. Vilgis, "Rheological study of the gelation process of agarose-based solutions", *Food Biophysics*, vol. 6, no. 4, p. 450, 2011, ISSN: 1557-1866. DOI: 10.1007/s11483-011-9225-0.

[28] M. Ahearne, Y. Yang, A. Haj, K. Then, and I. K.-K. Liu, "Characterizing the viscoelastic properties of thin hydrogel-based constructs for tissue engineering applications", vol. 2, pp. 455–63, Jan. 2006.

[29] C. D. Markert, X. Guo, A. Skardal, Z. Wang, S. Bharadwaj, Y. Zhang, K. Bonin, and M. Guthold, "Characterizing the micro-scale elastic modulus of hydrogels for use in regenerative medicine", *Journal of the Mechanical Behavior of Biomedical Materials*, vol. 27, pp. 115–127, 2013, ISSN: 1751-6161. DOI: https://doi.org/10.1016/j.jmbbm.2013.07.008.

[30] P. Aymard, D. R. Martin, K. Plucknett, T. J. Foster, A. H. Clark, and I. T. Norton, "Influence of thermal history on the structural and mechanical properties of agarose gels", *Biopolymers*, vol. 59, no. 3, pp. 131–144, DOI: 10.1002/1097-0282(200109)59:3<131::AID-BIP1013>3.0.CO;2-8.

[31] M. Watase, K. Nishinari, P. A. Williams, and G. O. Phillips, "Agarose gels: Effect of sucrose, glucose, urea, and guanidine hydrochloride on the rheological and thermal properties", *Journal of Agricultural and Food Chemistry*, vol. 38, no. 5, pp. 1181–1187, 1990.

[32] H. Ogura and Y. Yoshida, "Cavity theory of fabry perot resonator", *Japanese Journal of Applied Physics*, vol. 3, no. 9, p. 546, 1964.

Chapter 7

Appendices

7.1 Summary of Collected Data

	Water	Modulus (MPa)	S11
Agarose ↑	↓	↑ 0.03 ± 0.0009	↓ -18.3 ± 14.7
		0.08 ±0.02	-7.8 ± 0.06
		0.04 ± 0.002	-8.7 *
		0.03 ± 0.005	-9.3 ± 0.1
Glucose ↑	↓	↓ 0.009 ± 0.0009	↓ -9.26 ± 0.09
		0.005 ± 0.0005	-9.08 ± 0.04
		0.008 ± 0.001	-8.40 ± 0.2
		0.02 ± 0.004	-6.56 ± 0.06
		0.04 ± 0.004	-6.71 ± 0.03
Thickness ↑	↓	13.1 ± 5.4	-14.8 ±4.5
		4.9 ± 1.3	-6.1 ± 0.6
		15.7 ± 5.2	-10.7 ± 0.009
		4.5 ± 0.2	-9.1 ± 2.7
		2.0 ± 0.5	-9.3 ± 0.1

FIGURE 7.1: Summary of collected data from Texture and RF analyses

7.2 Safety

HAZOP Analysis:

Potential Hazards	Consequences	Safe Guards	Actions
Hot Surfaces (Heating Bath plate)	If not handled with care may cause burns	Use appropriate PPE	Run cold water over burnt area for 10 mins
Sharp probe in Texture Analyser	Hand injuries	Avoid putting hand under probe when the Texture Analyser is running	First aid kit loca
Solution spillage	Can cause damage to electrical devices in the room, toxic fumes, potential fire hazard	Make sure solutions are covered when transporting from one place to another or when not in use, do not place chemical where it can be easily knocked over	Shut off electronic device that has been spilled on, absorb immediately with an inert material if small spill or use water and mop up depending on chemical's solubility in water (toluene is almost insoluble in water). If large spill, absorb with DRY earth, sand or other non-combustible material
N_2 gas tank leakage/explosion	oxygen-depleted environment: non-breathable, explosion of compressed gas could lead to fatality	Ensure that valves are opened slowly to prevent damage in regulator, Do not tamper with safety valves, ensure that gas cylinder is upright and safely attached to wall, Avoid applying large force to cylinder	DO NOT enter room if leakage occurs, Inform lab manager

7.2.1 Material Safety Data Sheets

- Agarose
- Glucose
- Water